International Journal of Biological Macromolecules 253 (2023) 126718

Contents lists available at ScienceDirect

International Journal of Biological Macromolecules

journal homepage: www.elsevier.com/locate/ijbiomac

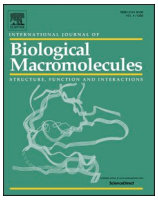

Preparation of injectable porcine skin-derived collagen and its application in delaying skin aging by promoting the adhesion and chemotaxis of skin fibroblasts

He Ni [a,b,1], Chao Liu [a,1], Lili Kong [b,1], Limin Zhai [a], Jiapeng Chen [a], Qingpeng Liu [a], Zhendong Chen [a], Mengdie Wu [a], Jie Chen [a], Yiyan Guo [a], Weiwei Bai [a], Dandan Zhang [a], Kunwen Xia [a], Guowei Huang [a], Shengjun Pan [a], Beining Liao [a], Kuo Ma [a], Ling-Kun Zhang [a,c,d,*], Jian Cheng [b,*], Yan-Qing Guan [a,c,d,*]

[a] School of Life Science, South China Normal University, Guangzhou 510631, China
[b] Chongqing Fanghe Biotechnology Co., LTD, Chongqing 400000, China
[c] South China Normal University-Panyu Central Hospital Joint Laboratory of Translational Medical Research, Panyu Central Hospital, Guangzhou 511400, China
[d] MOE Key Laboratory of Laser Life Science & Institute of Laser Life Science, Guangdong Provincial Key Laboratory of Laser Life Science, Guangzhou Key Laboratory of Spectral Analysis and Functional Probes, College of Biophotonics, South China Normal University, Guangzhou 510631, China

ARTICLE INFO

Keywords:
Collagen
Cell chemotaxis
Cell adhesion
Delaying senescence

ABSTRACT

Collagen, as the main component of human skin, plays a vital role in maintaining dermal integrity. Its loss will lead to dermis destruction and collapse, resulting in skin aging. At present, injection of exogenous collagen is an important means to delay skin aging. In this study, high-purity collagen was extracted from porcine skin. Our research revealed that it can effectively promote the adhesion and chemotaxis of HSF cells. It can also reduce the expression of β-galactosidase, decrease ROS levels, and increase the expression of the collagen precursors, p53 and p16 in HSF cells during senescence. After local injection into the aging skin of rats, it was found that the number of cells and type I collagen fibers in the dermis increased significantly, and the arrangement of these fibers became more uniform and orderly. Moreover, the important thing is that it is biocompatible. To sum up, the porcine skin collagen we extracted is an anti-aging biomaterial with application potential.

1. Introduction

Collagen, one of the most abundant proteins in the human body, is widely distributed in the connective tissue, skin, bone, visceral cell stroma and other tissues [1]. It plays a crucial role in supporting organs, protecting the body, and is closely associated with physiological activities such as tissue formation, maturation, cell differentiation and calcification [2]. Therefore, collagen has garnered increasing interest as an important biomaterial for tissue engineering and regenerative medicine.

Collagen accounts for 85–90 % of the dry weight of skin and is essential for maintaining skin elasticity [3,4]. However, during the aging process, various changes occur, including the appearance of a rough texture, wrinkles, spots, and atrophy, leading to a loss of skin tissue integrity [5,6]. Due to the destruction of collagen fibers, fragmented collagen fibers accumulate in the extracellular matrix [7,8]. Then, the collagen may show progressive cross-linking and calcification, making the skin lose elasticity [9,10]. The ability of fibroblasts to synthesize collagen was gradually reduced, leading to the destruction and collapse of the extracellular matrix, and skin aging [11,12].

In addition, skin aging is accompanied by the activation of inflammatory responses in skin tissues [13]. Inflammatory factors are secreted by immune cells, such as mast cells and macrophages, which destroy collagen in the skin [14]. Furthermore, these inflammatory factors accelerate the aging of cells and the destruction of extracellular matrix in the skin tissue. Additionally, cell senescence or apoptosis in skin tissue might directly disrupt the balance of tissue degradation and regeneration [15,16]. Therefore, collagen plays a central role in maintaining the topography and histological structure of the skin, combating skin aging.

Numerous studies have indicated that fibroblasts are closely related

* Corresponding authors at: School of Life Science, South China Normal University, Guangzhou 510631, China.
E-mail addresses: lkzhang@m.scnu.edu.cn (L.-K. Zhang), 13905712012@163.com (J. Cheng), guanyq@scnu.edu.cn (Y.-Q. Guan).
[1] These authors contributed equally to this work and should be considered co-first authors.

https://doi.org/10.1016/j.ijbiomac.2023.126718
Received 12 June 2023; Received in revised form 18 August 2023; Accepted 3 September 2023
Available online 7 September 2023

to the renewal and repair of collagen through the secretion of matrix metalloproteinases (MMPs) and tissue inhibitors of metalloproteinases (TIMPs) [17], which maintain skin elasticity and firmness, respectively [18,19]. Collagen exhibits close interactions with skin cells, significantly influencing cell adhesion, migration, morphology, proliferation, differentiation, and the regulation of inflammation, among other cellular behaviors [20,21]. Furthermore, collagen could promote cell survival, adhesion and migration through activation of Erk1/Erk2 (p44/42) mitogen-activated protein kinase (MAPK) signal transduction pathway. Therefore, shaping a biomimetic microenvironment through collagen implantation to promote skin repair and regeneration was very important [22].

Additionally, recent studies have shown that, collagen can stimulate dermal fibroblasts to produce new collagen to repair skin tissues [23,24]. Meanwhile, collagen is highly conserved in biological evolution, so porcine skin-derived collagen is highly homologous to human collagen [25,26]. Therefore, the immunogenicity of porcine skin-derived collagen is extremely low, with high safety and biocompatibility [27]. Recent studies have shown that highly purified and sterilized porcine skin-derived collagen molecules stabilize loose collagen molecules during the construction of implants, creating a strong and transparent material [28]. It has been applied in clinical studies to affordably handle and implant eyes as a replacement for human corneas. Moreover, the ease of obtaining porcine skin-derived collagen makes it economically advantageous, thereby expanding its potential market applications.

Here, we developed and validated a simple and efficient procedure to prepare high-purity collagen from porcine skin. Then, the effect of prepared collagen on skin cell adhesion and chemotaxis was investigated to clarify the mechanism by which skin aging is delayed. Our results provide a theoretical basis for the application and functional research of porcine skin-derived collagen in the medical and cosmetic industries.

2. Materials and methods

2.1. Material and reagents

SPF porcine skin was purchased from Chongqing Academy of Animal Sciences. Pepsin, collagenase and Mini-Protean TGXTM precast gel were purchased from Yuanye Biotechnology (Shanghai, China), and HPLC solvents were procured from Burdick & Jackson (Muskegon, MI, USA). Other solvents and reagents, which were analytical grade, were purchased from local suppliers.

2.2. Preparation of collagen from porcine skin

Fresh porcine skin was dissected into 5 mm × 5 mm after removing subcutaneous fat. Then the skin was defatted with 5 % Na_2CO_3 at a sample/solution ratio of 1:20 (w/v). The mixture was stirred for 3 h, and 5 % Na_2CO_3 solution was changed every 1 h. Defatted skin was washed with distilled water three times. For removal of soluble protein, defatted skin was smashed in a Juicer followed by homogenized using an Ultra-turrax T18 blender (IKA, Staufen, Germany) for 2 min at 10,000 rpm with 50 mL phosphate buffer saline (PBS, pH 6.8) and extracted for 30 min with stirring at 4 °C.

After centrifugation for 20 min at 8000 rpm and washed using distilled water, the precipitated collagen was dissolved in 50-fold of 0.5 mol/L acetic acid solution containing 1/50 (w/w) of pepsin overnight at 25 °C. Then the supernatant was adjusted to neutrality by adding NaOH solution to reconstitute and deactivating enzyme. The coagulated collagen was washed using Millipore water to purify it.

2.3. Physicochemical properties of collagen

2.3.1. Purity determination of collagen SDS-PAGE analysis

The purity of porcine collagen was determined by SDS-PAGE according to Pharmaceutical industry standard of the People's Republic of China (YY/T 1453–2016). Collagen was dissolved at 1 mg/mL using 3 mol/L acetic acid solution as sample A. Meanwhile, equal amount of collagen was hydrolyzed by collagenase for 4 h at 37 °C (sample B), and the collagenase solution was sample C. Three samples were subjected to SDS-PAGE on a 4–20 % Mini-Protean TGXTM precast gel. Electrophoretic migration was performed at 150 V (constant) for 40 min. The resulting gels were stained, destained and scanned according to Carvalho's method [29]. Alpha View integration software was used to quantify percent area for each band in three samples. The purity of collagen was calculated as follows:

$$\text{Purity of collagen}\ (\%) = \mathrm{A} - (\mathrm{B} - \mathrm{C}) \times 100\%$$

In this equation: A is collagen dissolved at 1 mg/mL using 3 mol/L acetic acid solution, B is equal amount of collagen hydrolyzed by collagenase for 4 h at 37 °C, and C is the collagenase solution.

2.3.2. LC-MS/MS analysis

Purified collagen was mixed with 200 μL of 8 M urea in Nanosep Centrifugal Devices (PALL). The device was centrifuged at 12,000 *g* at 20 °C for 20 min. Then, 200 μL of 8 M urea solution with 10 mM DTT were added, and the reduction reaction was kept for 2 h at 37 °C. The solution was removed by centrifugation, and 200 μL 8 M urea solution with 50 mM iodoacetamide (IAA) was added. The sample was incubated in the dark for 15 min at room temperature. The ultra-fraction tube was washed with 200 μL of 8 M urea three times and 200 μL of 25 mM ammonium bicarbonate three times by centrifugation at 12,000*g* for 20 min at room temperature. Then, 100 μL of 25 mM ammonium bicarbonate containing 0.01 μg/μL trypsin was added to each filter tube. The tubes were incubated at 37 °C for 12 h. The filter tubes were washed twice with 100 μL of 25 mM ammonium bicarbonate by centrifugation 12,000*g* for 10 min. The flow-through fractions were collected and lyophilized.

The lyophilized peptide fractions were resuspended in double-distilled water containing 0.1 % formic acid, and 2 μL aliquots of which was loaded into a nanoViper C18 (Acclaim PepMap 100, 75 μm × 2 cm) trap column. The online Chromatography separation was performed on the Easy nLC 1200 system (ThermoFisher). The trapping, desalting procedure were carried out with a volume of 20 μL 100 % solvent A (0.1 % formic acid). Then, an elution gradient of 5–38 % solvent B (80 % acetonitrile, 0.1 % formic acid) in 60 min was used on an analytical column (Acclaim PepMap RSLC, 75 μm × 25 cm C18–2 μm 100 Å). DDA (data-dependent acquisition) mass spectrum techniques were used to acquire tandem MS data on a ThermoFisher Q Exactive mass spectrometer (Thermo Fisher, USA) fitted with a Nano Flex ion source. Data was acquired using an ion spray voltage of 1.9 kV, and an interface heater temperature of 275 °C. For a full mass spectrometry survey scan, the target value was 3×10^6 and the scan ranged from 350 to 2000 *m/z* at a resolution of 70,000 and a maximum injection time of 100 ms. For the MS/MS scan, only spectra with a charge state of 2–5 were selected for fragmentation by higher-energy collision dissociation with a normalized collision energy of 28. The MS/MS spectra were acquired in the ion trap in rapid mode with an AGC target of 8000 and a maximum injection time of 50 ms. Dynamic exclusion was set for 25 s.

The MS/MS data were analyzed for protein identification and quantification using PEAKS Studio 8.5. The local false discovery rate at PSM was 1.0 % after searching against *Sus scrofa* database with a maximum of two missed cleavages. The following settings were selected: Oxidation (M), acetylation (Protein N-term), deamidation (NQ), Pyro-glu from E, Pyro-glu from Q for variable modifications as well as fixed carbamidomethylation of cysteine. Precursor and fragment mass tolerance were set to 10 ppm and 0.05 Da, respectively.

2.4. Cell experiment

2.4.1. Cell culture

HaCaT cells and HSF cells from Shenzhen Institute of Advanced Technology, Chinese Academy of Sciences were cultured in DMEM high glucose medium (containing 10 % fetal bovine serum and 1 % penicillin-streptomycin mixed double antibody). The culture conditions were as follows: 37 °C, 5.0% CO_2 constant temperature and humidity incubator.

2.4.2. Cell cytotoxicity test

The cytotoxicity of porcine skin collagen was detected by CCK-8 method. HaCaT cells and HSF cells in good growth condition were digested with trypsin and inoculated in 96-well plate at the density of 2 $\times$ 10^5 cells/mL for 24 h, with 4 parallel holes in each group. The cells were treated with different concentrations of porcine skin collagen (0.3, 0.6, 0.9, 1.2, 1.5 mg/mL) for 24 h. 100 μL CCK-8 working solution (90 μL DMEM + 10 μLCCK-8) was added to each well and incubated in cell incubator for 3 h. The CCK-8 working solution was sucked out and centrifuged to remove the residual collagen. 80 μL working solution was added to the new 96-well plate, and the absorbance value (OD) at 450 nm was detected by enzyme labeling instrument.

2.4.3. Cell adhesion

HaCaT and HSF cells in logarithmic growth phase were inoculated in 96-well plate at the concentration of 2 $\times$ 10^5 cells/mL. The cells in the experimental group were diluted with medium containing different concentrations of porcine skin collagen, and the negative control group was diluted with complete culture medium. After 4 h of cell culture (that is, the cell adhesion time), the cells were treated with CCK-8 working solution for 3 h. The CCK-8 working solution was gently sucked out and centrifuged to remove residual collagen. 80 μL working solution was added to the new 96-well plate, and the absorbance value (OD) at 450 nm was detected by enzyme labeling instrument.

2.4.4. Tanswell

HSF cells in logarithmic growth phase were selected and cultured in serum-free medium overnight, which made the cells hungry. The complete medium containing different concentrations of porcine skin collagen (0.3, 0.6, 0.9 mg/mL) was added to the 24-well plate, and the cell suspension diluted with serum-free medium was added to the Tanswell chamber to shake gently so that the cells were evenly distributed. Pay attention to no air bubbles at the bottom of the compartment, and the Tanswell chamber was cultured in the orifice plate for 24 h. After fixing the cell 15 min with 4 % paraformaldehyde, the cells were stained with crystal purple dye, the unmigrated cells in the chamber were erased with a cotton swab, and the inverted chamber was naturally air-dried at room temperature. Under the microscope, 3 visual fields were taken from each hole. The cells were counted by ImageJ software.

2.4.5. Construction of senescence model of HSF cells

HSF cells with good growth condition were inoculated in 6-well plates for overnight culture. The cells were treated with different concentrations of D-galactose (10, 20, 30, 50 mg/mL) for 24 h. 1 mL staining fixative was added to each hole, 15 min was fixed at room temperature, PBS was used to clean the cells for 3 times, and 1 mL staining working solution (A:B:C:X-gal = 1:1:93:5) was added to each well. The culture plate was incubated overnight in a 37 °C incubator (without CO_2), and three visual fields were taken under microscope.

Then, HSF cells with good growth condition were inoculated in 96-well plates for overnight culture. The cells were treated with different concentrations of D-galactose (10, 20, 30, 50 mg/mL) for 24 h. CCK-8 working solution was added to each hole and incubated in the incubator for 3 h. The absorbance value (OD) at 450 nm was detected by enzyme labeling instrument.

2.4.6. Detection of the changes of intracellular β-galactosidase

HSF cells in good growth condition were cultured overnight, the negative control group (Control) was added with complete medium, the model group (D-Gal) was added with complete medium containing 20 mg galactose, and the experimental group (D-Gal+ColI) was added with complete medium containing 20 mg LLD-galactose and 600 μg/mL porcine skin collagen homogenate. The positive control group (D-Gal+Coll III) was added with recombinant typeIII collagen fiber containing 20 mg Gal-galactose and 600 μg/mL. The cells were cultured for 24 h. Wash the collagen in the experimental group. 1 mL staining solution was added to each hole, 15 min was fixed at room temperature, and 1 mL staining solution (A:B:C:X-gal = 1:1:93:5) was added to each hole. The culture plates were incubated overnight at 37 °C. The culture plates were photographed under microscope and three visual fields were taken.

2.4.7. Detection of ROS expression in cells

HSF cells in good growth condition were cultured overnight. As mentioned earlier, the experiment was divided into four groups with 3 double holes in each group. After the culture plate was placed in the cell incubator and cultured for 24 h, the DCFH-DA probe diluted in serum-free medium was used, and 0.5 mL was added to each well. After incubating in the cell incubator for 30 min, 0.5 mL was added to wash the excess probe, 0.5 mL Hoechst33342 (4 μg/mL) was added, 15 min was co-incubated with cells, cells were washed twice, PBS of 0.5 mL was added, and the fluorescence intensity was recorded by putting it under an inverted fluorescence microscope. It should be noted that the operation of avoiding light is carried out throughout the whole process from the incubation of the probe.

The senescence of HSF cells will affect the expression of collagen, that is, the production level of collagen precursor. ELISA (enzyme-linked immunosorbent assay) was used to detect the effect of porcine skin collagen on the level of collagen precursor in aging HSF cells. HSF cells in good growth condition were inoculated in 24-well plates and cultured overnight. The cells were divided into four groups. After the cells were cleaned, 100 μL cell lysate was added, and the culture plate was placed on ice to cleave the cell 20 min (shaker, 50 rpm). The lytic cells were blown and mixed and collected into the EP tube, centrifuged at 5000 rpm at 4 °C for 5 min, and the supernatant was sucked out and transferred to the new EP tube. The collected samples were operated according to the instructions of ELISA kit. The absorbance at 450 nm wavelength was measured by enzyme labeling instrument, and the content of collagen in HSF extracellular matrix was calculated according to the standard curve drawn.

2.4.8. Immunofluorescence

The HSF cells in good growth condition were inoculated into the 6-well plates which had been put into the cell climbing slices, and 3 compound holes in each group were cultured overnight. Experimental grouping and treatment, as mentioned earlier, the cells were washed after 24 h of incubation. 20 min was fixed on the shaker with cell fixing liquid. After cleaning, 100 μL membrane-breaking working solution was added and incubated for 20 min at room temperature. 5 min was washed for 3 times, and the cells were evenly covered with 3%BSA. 30 min was sealed at room temperature. After clearing the sealing solution, diluted (PBS, 1:200) p53 mouse monoclonal antibody and p16 rabbit monoclonal antibody were added to the orifice plate and incubated in refrigerator at 4 °C for the night. After shaking and washing on the shaker for 3 times, FITC-labeled sheep-anti-mouse and Cy3-labeled sheep-anti-rabbit secondary antibody covering cells were added respectively to incubate 50 min. Remove the fluorescent second antibody and wash the cells, add DAPI working solution, and incubate 10 min at room temperature without light. Add anti-fluorescence quenching and seal the tablets, observe and take pictures under the fluorescence microscope.

2.4.9. Western blotting

The HSF cells in good growth condition were cultured in the incubator overnight. The four groups of cells were treated as above, washed and collected into EP tube. The RIPA protein lysate 1 mL (containing 10 μ L proteasome inhibitor) was added and placed on the ice pipette to repeatedly blow and lyze 30 min to make the cells lytic completely. 10 min was centrifuged with cryogenic centrifuge 12,000 rpm, the supernatant was collected, and the protein concentration was determined according to the instructions of BCA kit. 10 % of the lower separation gel and 5 % of the upper concentrated gel were prepared, the sample amount of each pore protein was 10 μL, the glue was covered with PVDF membrane (polyvinylidene fluoride film), the film was transferred at low temperature, the 30 min was sealed with 5 % skimmed milk powder on the shaker at room temperature, and then p53 and p16 mouse monoclonal antibodies (diluted by PBS 1:1000) were added respectively, and incubated overnight at 4 °C. Clean the membrane with TBST for 3 times (5 min each time). Add the second antibody (goat anti-mouse) and incubate at room temperature for 2 h. The membrane was also cleaned with TBST for 3 times (5 min each time). The exposure solution ECL was uniformly coated on the PVDF film, and the band information was detected in the gel imaging system. The target strip is analyzed by ImageJ software, and the statistical result of strip gray value is obtained. β-Actin was used as the standardized internal reference of the protein, and the ratio of the target protein to the internal reference protein was used as the relative expression of the target protein.

2.5. Animal studies

2.5.1. Construction and grouping treatment of aging model in rats animal feeding

Eight SPF SD rats (Guangdong Medical Experimental Animal Center) were selected, half male and half female. The weight of female rat was 130 g–160 g and that of male rat was 150 g–180 g. The temperature of the animal room is 20–26 °C, the relative humidity is 40 %–70 %, the light is light and dark for 12 h, and the minimum number of ventilation is 15 times per hour. Keep the animals free in the course of feeding.

Eight rats were raised in a standardized animal room with constant temperature and ventilation, provided with sufficient food and pure water, and the rats were fed for 24 months to make them senile normally. Ten local injection sites were selected on both sides of the back spine of each rat for local treatment of aging skin. 200 μL porcine skin collagen homogenate containing 1 mg/mL and 3 mg/mL was injected into the experimental group, and the same amount of normal saline was injected into the control group. Three sites were injected into each group. The changes of skin were detected after one month. Then, SD rats were weighed every three days after injection of collagen. Seven days after injection of collagen, 2 mL was collected from rat tail vein and placed in EDTA anticoagulant tube. The changes of blood indexes in rats were detected by automatic blood cell counter.

2.5.2. H&E staining and Masson staining of rat skin

One month after the intervention of collagen injection, the rats were euthanized with pentobarbital sodium (50 mg/kg). The skin around the injection site on the back of the rats and the heart, liver, spleen, lung and kidney of the rats were dissected completely, the blood stains were cleaned with PBS, placed in the 50 mL centrifuge tube, and fixed with 4 % paraformaldehyde for >24 h. Take out the scalpel and trim it, put it in the embedding frame and mark it. The dehydration box was put into a dehydrator, soaked in 75 % alcohol, 85 % alcohol, 90 % alcohol and 95 % alcohol for 4 h, 2 h and 1 h, then soaked in anhydrous ethanol twice (each time 30 min), and then successively immersed in alcoholic benzene and xylene 5–10 min to dehydrate the tissue, and the dehydrated tissue was immersed in a pre-melted paraffin solution (paraffin I: paraffin II:paraffin III = 1:1:1) 40 min. Put the melted wax into the embedding frame, and put the tissue soaked in the wax into the embedding frame in accordance with the requirements of the embedding surface. It is placed on the freezing table to cool at −20 °C, and the wax block is repaired after solidification. The repaired wax blocks were placed on a paraffin slicer with a thickness of 4 μm. The slices float on the 40 °C warm water in the spreading machine, flatten the tissue, pick up the slides, dry the water in the oven at 60 °C and remove the wax, remove and store at room temperature.

The paraffin sections of 2.5.5 rat skin, heart, liver, spleen, lung and kidney were dewaxed twice in an environmentally friendly dewaxing solution (each 20 min), then soaked in anhydrous ethanol and 75 % alcohol each 5 min, washed twice with anhydrous ethanol, and finally washed with ultra-pure water. The treated slides were immersed in hematoxylin dye solution for 3–5 min, the excess dye solution was washed with ultra-pure water, differentiation solution was added, differentiation solution was washed, PBS was added back to blue 1 min, and 5 min was washed with ultra-pure water. The slides were then immersed in 85 % and 95 % alcohol gradient dehydration of each 5 min, then dyed 5 min in eosin dye solution, washed the glass slides 3 times with ultra-pure water, and removed the excess eosin dye solution. The slides were dehydrated with anhydrous ethanol for 3 times, each time 5 min, and then washed with xylene twice (each 5 min) for transparent operation. Add neutral gum and cover the cover glass to seal the sheet to avoid bubbles and dry overnight. The positive fluorescence microscope was used to observe and collect the image.

The rat skin slices made by 3.2.5 were dewaxed twice in an environmental dewaxing solution (each 20 min), then soaked in anhydrous ethanol and 75 % alcohol each 5 min, washed twice with anhydrous ethanol, each 5 min, and finally washed with ultra-pure water. The treated slides were immersed in Masson A solution overnight and washed with ultra-pure water for 3 times. Continue to soak the slides into the mixture of Masson B solution and Masson C solution (the mixing ratio is 1:1) to dye 1 min, wash the slides with ultra-pure water, add differentiation solution to differentiate, and rinse the differentiation solution. Then put the slide into Masson D solution to dye 6 min and rinse it with ultra-pure water. Then use Masson E solution to dye 1 min around. Note that there is no cleaning here, wait for the E solution to drain slightly, then directly dip it into the Masson F solution for 2–30 s. The slices were then rinsed and differentiated with 1 % acetic acid. The slides were dehydrated with anhydrous ethanol for 3 times, each time 5 min, and then washed with xylene twice (each 5 min) for transparent operation. Add neutral gum and cover the cover glass to seal the sheet to avoid bubbles and dry overnight. The positive fluorescence microscope was used to observe and collect the image.

2.5.3. Sirius red staining of rat skin

The rat skin slices made by 3.2.5 were dewaxed twice in an environmental dewaxing solution (each 20 min), then soaked in anhydrous ethanol and 75 % alcohol each 5 min, washed twice with anhydrous ethanol, each 5 min, and finally washed with ultra-pure water. The treated slides were immersed in Sirius scarlet dye solution for 8 min staining. The slides were dehydrated with anhydrous ethanol for 3 times, each time 5 min, and then washed with xylene twice (each 5 min) for transparent operation. Add neutral gum and cover the cover glass to seal the sheet to avoid bubbles and dry overnight. Use polarized light microscope to observe and collect images.

2.6. Data analysis

The experimental results are analyzed by GraphPad Prism 8.0 software. In order to detect the differences between different groups, the independent sample *t*-test was used to analyze the variance of the experimental results. It was considered statistically significant when $p < 0.05$ ($0.01 < {}^{*}p < 0.05$, $0.001 < {}^{**}p < 0.01$, ${}^{***}p < 0.001$).

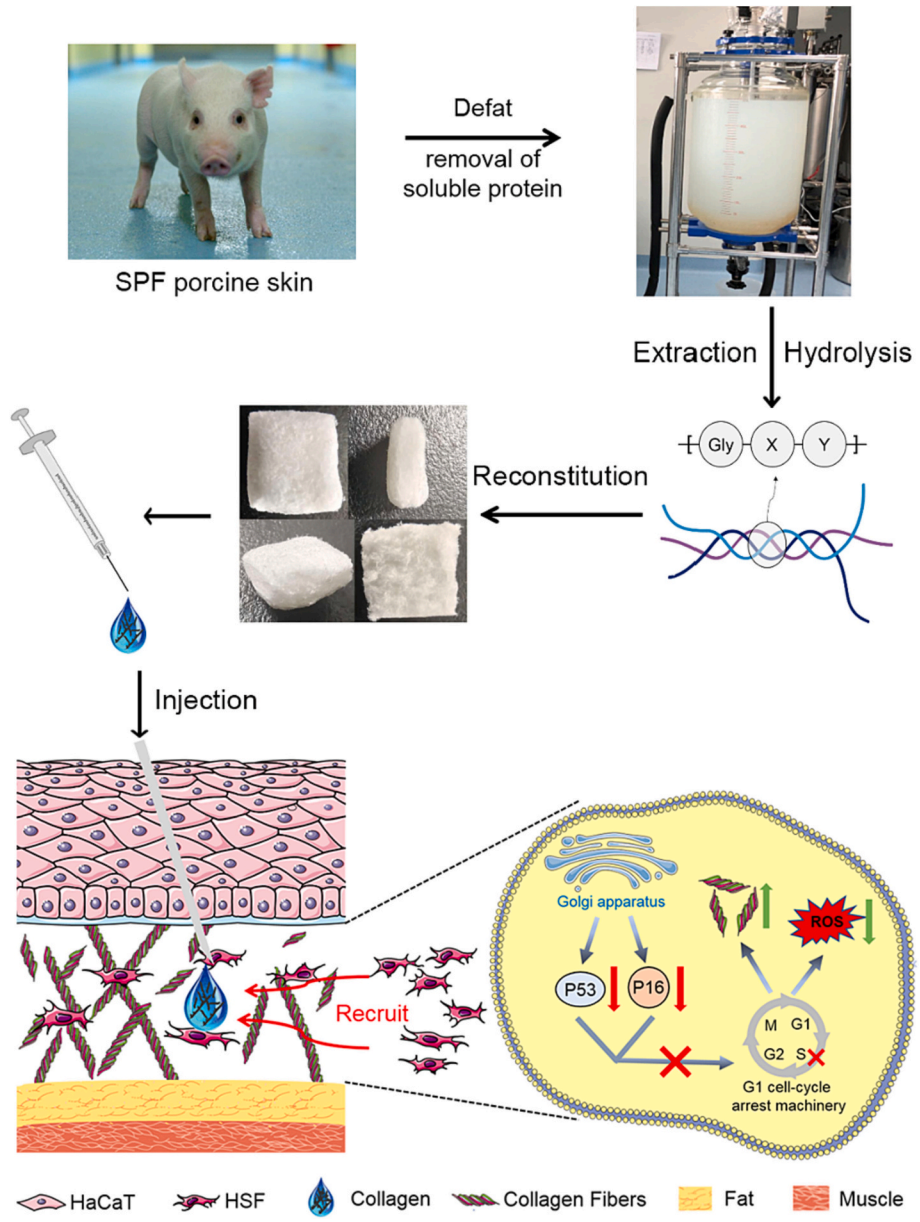

Fig. 1. Extraction and purification of collagen from pig skin and its effect on skin cell adhesion and chemotaxis and the mechanism of delaying skin aging.

3. Results and discussion

3.1. Preparation of collagen from porcine skin

It has been claimed that the immunogenicity and antigenicity of collagen are mainly attributed to the terminal telopeptides [27]. Therefore, pepsin in acetic acid solution was used to hydrolyze collagen to produce atelocollagen from porcine skin after defatting and removal of soluble protein. As shown in Fig. 1A, α1 and α2 chains (with about 130 kDa), β11 and β12 chains, and small amounts of γ chain were detected using SDS-PAGE, which was consistent with the literature [30,31]. According to YY/T 1453-2016, the purity of collagen was over 99 %, and the telopeptide fragments could not be detected by LC-MS/MS (Fig. 2B & C). Although previous studies have investigated the preparation process of collagen, high-purity atelocollagen has not yet been produced [30]. The preparation method mentioned used here is simple and environmentally friendly.

3.2. Cytotoxicity of collagen

Keratinocytes and fibroblasts, major cells in the skin tissue, play important roles granulation tissue formation and extracellular matrix synthesis [32]. In the present study, the CCK-8 assay was used to determine the toxicity of prepared collagen [33]. As shown in Fig. 3A & B, the proliferation rates of HaCaT and HSF cells treated with porcine skin collagen were not significantly different from those of control cells, which indicated that porcine skin collagen was not cytotoxic to HaCaT and HSF cells and had good biocompatibility and application potential.

3.3. Effect of collagen on cell adhesion and migration

To determine the effect of porcine skin collagen on the adhesion and migration of HaCaT and HSF cells, cells were treated with a medium containing 0, 0.3, 0.6, 0.9, and 1.2 mg/mL porcine skin collagen. As shown in Fig. 3D, after co-incubation for 4 h at concentrations of 0.3, 0.6, and 0.9 mg/mL, the number of adhered HSF cells was about 1.5 times higher than that of the control group, indicating that collagen

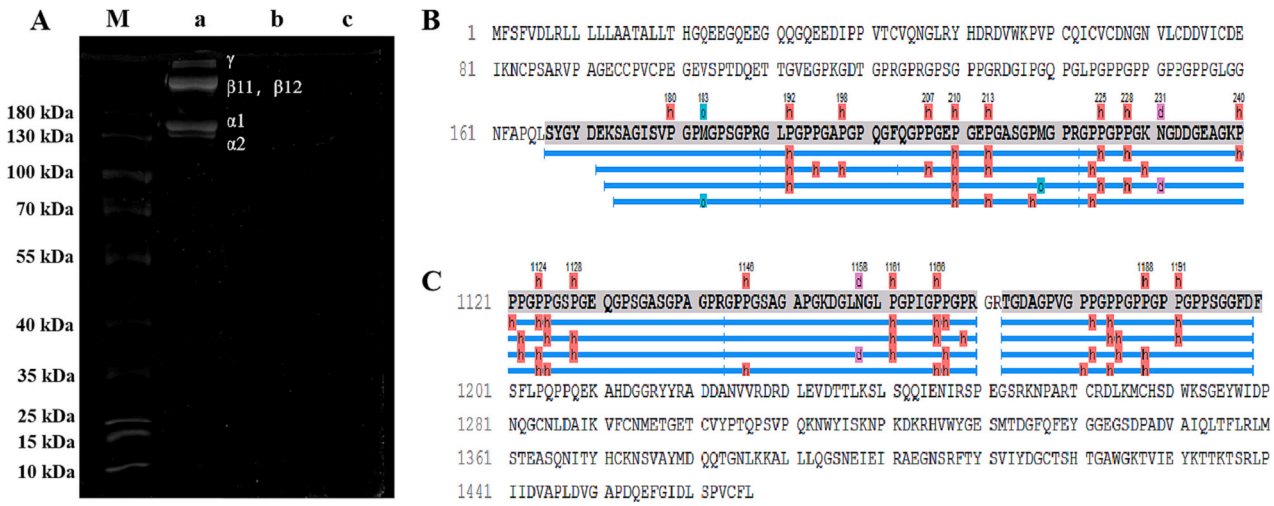

Fig. 2. (A) Detection of collagen structure of pigskin by SDS-PAGE. (B) Detection of porcine skin collagen telopeptide by LC-MS/MS.

could improve the adhesion of HSF cells. For HaCaT cells, after treatment with collagen, the number of adhered cells in each group was lower than that of the control group (Fig. 3C). The results showed that collagen promoted adhesion in HSF cells, but not in HaCaT cells. Therefore, injection of collagen into the dermis where fibroblasts are present may stimulate the adhesion of HSF cells.

Besides promoting cell adhesion, collagen could also impact the type, efficiency and direction of cell migration [34]. As shown in Fig. 3E, collagen significantly increased the number of migrated HSF cells, and the number of migrated HSF cells increased with the increase of collagen concentration. When the concentration of collagen was 0.6 mg/mL, compared with the control group, the number of migrated cells increased by about 40 %, and there was no significant difference between the 0.9 mg/mL group and the 0.6 mg/mL group. The results showed that collagen could effectively promote the migration of HSF cells.

3.4. Cell senescence model

The intracellular amount of senescence-associated β-galactosidase (SA-β-Gal), which gradually increases with the aging of cells, is often used as an index to determine whether cells are aging. SA-β-Gal can catalyze X-Gal to produce a blue-green color. HSF cells were treated with different concentrations of D-Gal for 24 h. The results showed that the proportion of SA-β-Gal-positive HSF cells was significantly higher in the experimental group than in the control group (Fig. 3F), suggesting that D-Gal can increase the expression of SA-β-Gal and induce senescence in HSF cells.

The proliferation of HSF cells after treatment with different concentrations of D-Gal was determined by the CCK-8 assay. As shown in Fig. 3G, colonization activity decreased gradually with the increase of D-Gal concentration, and the cell survival rate was decreased by about 50 % compared to the control group when the concentration of D-Gal was 20 mg/mL. Therefore, in the following experiments, the senescence model of HSF cells was established by stimulating HSF cells with 20 mg/mL D-Gal for 24 h.

3.5. Porcine skin collagen effectively delayed the senescence of HSF cells

The expression of SA-β-Gal increases with the aging of cells, and cell senescence can be monitored by staining the cells. As shown in Fig. 3H & I, in the negative control group, a very small number of slightly stained senescent cells were observed, while in the model group (D-Gal), about 70 % of the cells were senescent. After incubation for 24 h, the number of senescent cells was effectively reduced in the experimental group (D-Gal+Col I), and the number of positive cells was decreased by about 50 % compared with the model group. There was no significant difference in the number of senescent cells between the experimental group and the positive control group (D-Gal+Col III). The results showed that porcine skin collagen could effectively delay the senescence of HSF cells and exert an anti-aging effect.

3.6. Porcine skin collagen reduced the accumulation of ROS

The production of ROS is closely related to cell senescence. In the process of cell senescence, ROS accumulate in the cell, resulting in oxidative stress, a decline in cell vitality, and senescence. Intracellular ROS can react with DCFH-DA to produce DCF, which emits green fluorescence. As shown in Fig. 3J, the cells in the control group showed only weak fluorescence after co-incubation with the probe, while the cells in the model group (D-Gal) aged and emitted strong fluorescence, which proved that the senescent cells contained more ROS. The fluorescence intensity of the experimental group (D-Gal+Col I) was significantly lower than that of the model group. As shown in Fig. 3K, the fluorescence intensity decreased by about 50 %, and there was no significant difference compared with the positive control group (D-Gal+Col III). The results showed that the ROS levels were effectively reduced in the experimental group, that is, porcine skin collagen effectively delayed the senescence of HSF cells, reduced the accumulation of ROS in cells, and inhibited senescence.

3.7. Effect of porcine skin collagen on the expression of collagen precursors, p53 and p16

Reduced synthesis of dermal collagen is characteristic of chronologically aged skin [35]. Many factors affect the expression of collagen in HSF cells, which eventually lead to the senescence of skin HSF cells. To determine the effect of porcine skin collagen on HSF cell senescence, the expression of collagen precursors in D-Gal-induced senescence HSF cells was detected by ELISA. As shown in Fig. 4A, D-Gal could significantly decrease the production of collagen precursors and induce the senescence of HSF cells. After injection of porcine skin collagen (D-Gal+Col I) or the positive control (D-Gal+Col III), the expression levels of both collagen precursors were increased by about 100 % compared with the model group. The results indicated that porcine skin collagen could effectively promote the expression of intracellular collagen precursors, which can promote the regeneration of extracellular collagen and delay cell senescence.

In the process of cell senescence, multiple molecules and the corresponding signaling pathways are activated. The DNA damage response

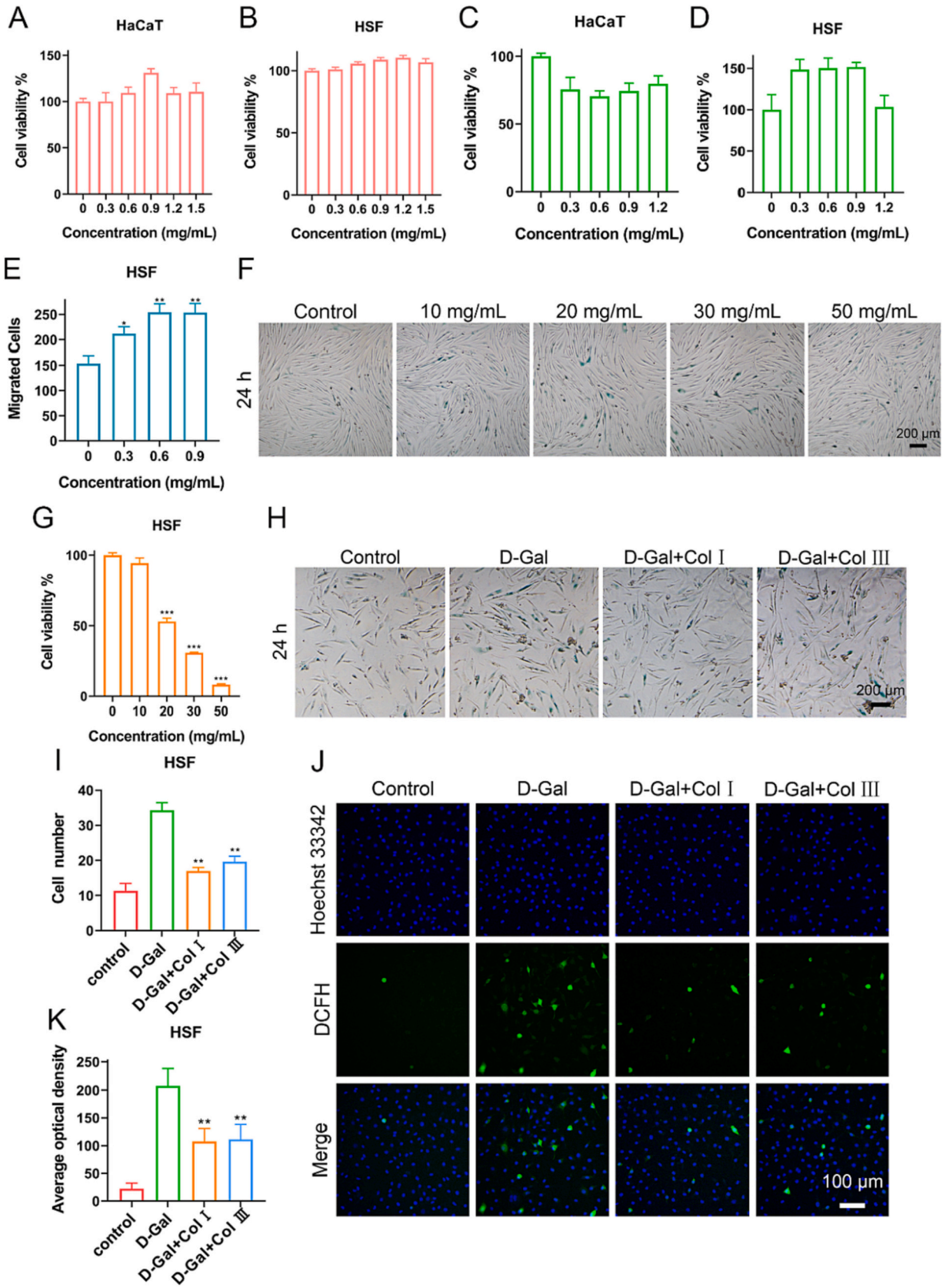

Fig. 3. Effect of porcine skin collagen on cells. The toxicity of different concentrations of porcine skin collagen to (A) HaCaT cells and (B) HSF cells was detected. Effects of different concentrations of porcine skin collagen on the adhesion of (C) HaCaT cells and (D) HSF cells. (E) The effect of porcine skin collagen on the migration of HSF cells was detected by Transwell ($n = 5$, $^{*}p < 0.05$ and $^{**}p < 0.01$). (F) β-Galactosidase staining and (G) D-galactose concentration analysis of cell model ($n = 5$, $^{***}p < 0.001$). (H) After collagen treatment, senescent HSF cells were stained and (I) quantitative analysis was performed ($n = 4$, $^{**}p < 0.01$). (J) The change of ROS fluorescence intensity after HSF cell treatment and (K) quantitative analysis ($n = 4$, $^{**}p < 0.01$).

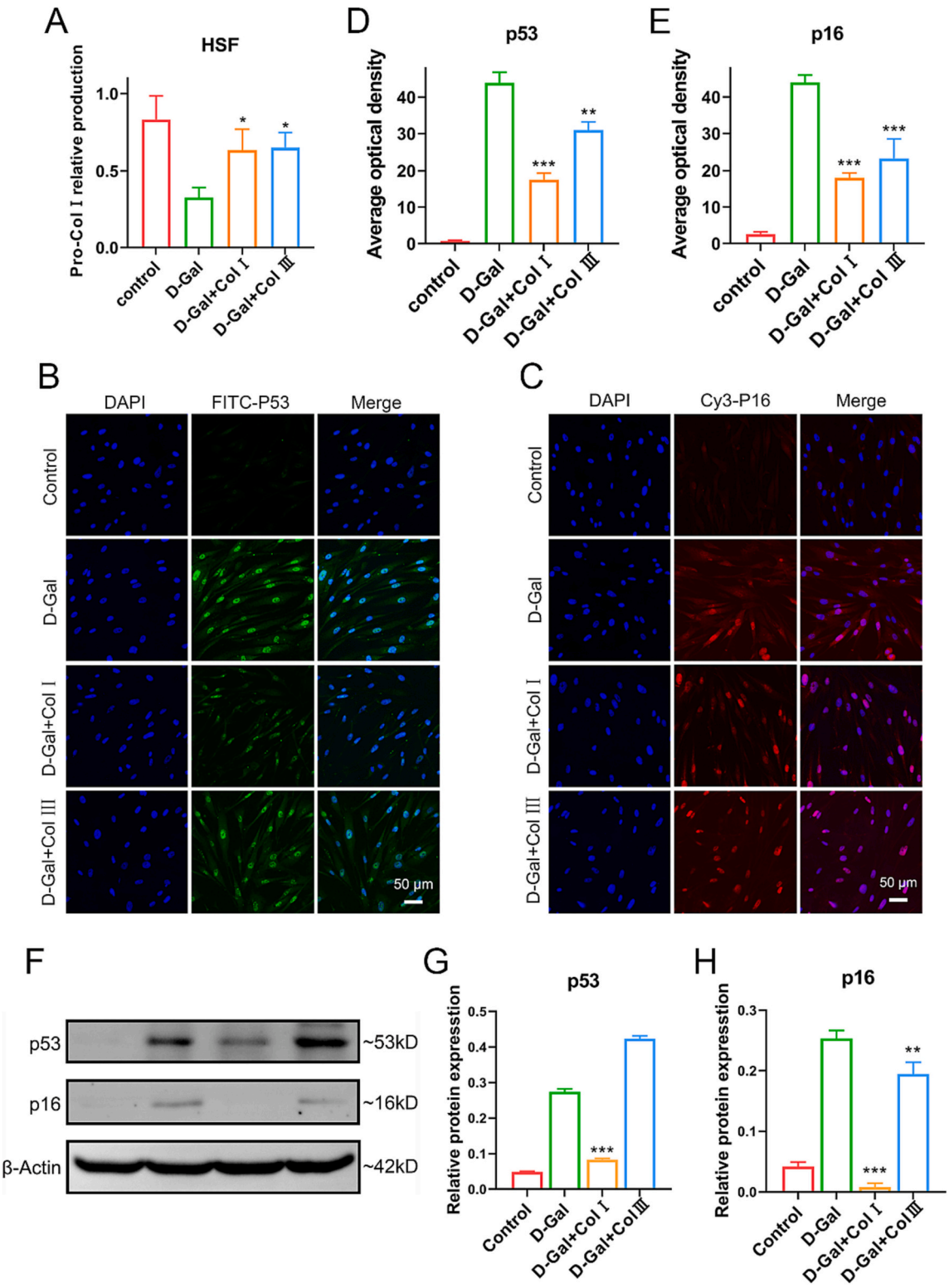

Fig. 4. (A) ELISA was used to detect the changes of type I collagen precursor in HSF cells after treatment ($n = 4$, $^{*}p < 0.05$). (B) The fluorescence intensity of p53 protein and (C) p16 protein in HSF cells was detected by immunofluorescence and (D) (E) quantitative analysis ($n = 4$, $^{**}p < 0.01$ and $^{***}p < 0.001$). (F) Western blot was used to detect the fluorescence intensity of p53 protein and p16 protein in HSF cells after treatment and (G) (H) quantitative analysis ($n = 4$, $^{**}p < 0.01$ and $^{***}p < 0.001$).

(DDR) and regulated cell cycle arrest are considered as important ways to regulate cellular senescence [36–38]. The DDR activates the MAPK signal cascade and the p53 pathway, and the production of the cell cycle inhibitor p16 leads to G1 cell cycle arrest and cell senescence [39,40]. As shown in Fig. 4B–E, the expression levels of p53 and p16 were significantly higher in the model group (D-Gal) than in the control group after 24 h of treatment, and Col I and Col III were both lowered the expression of p53 and p16 in the experimental group and the positive control group.

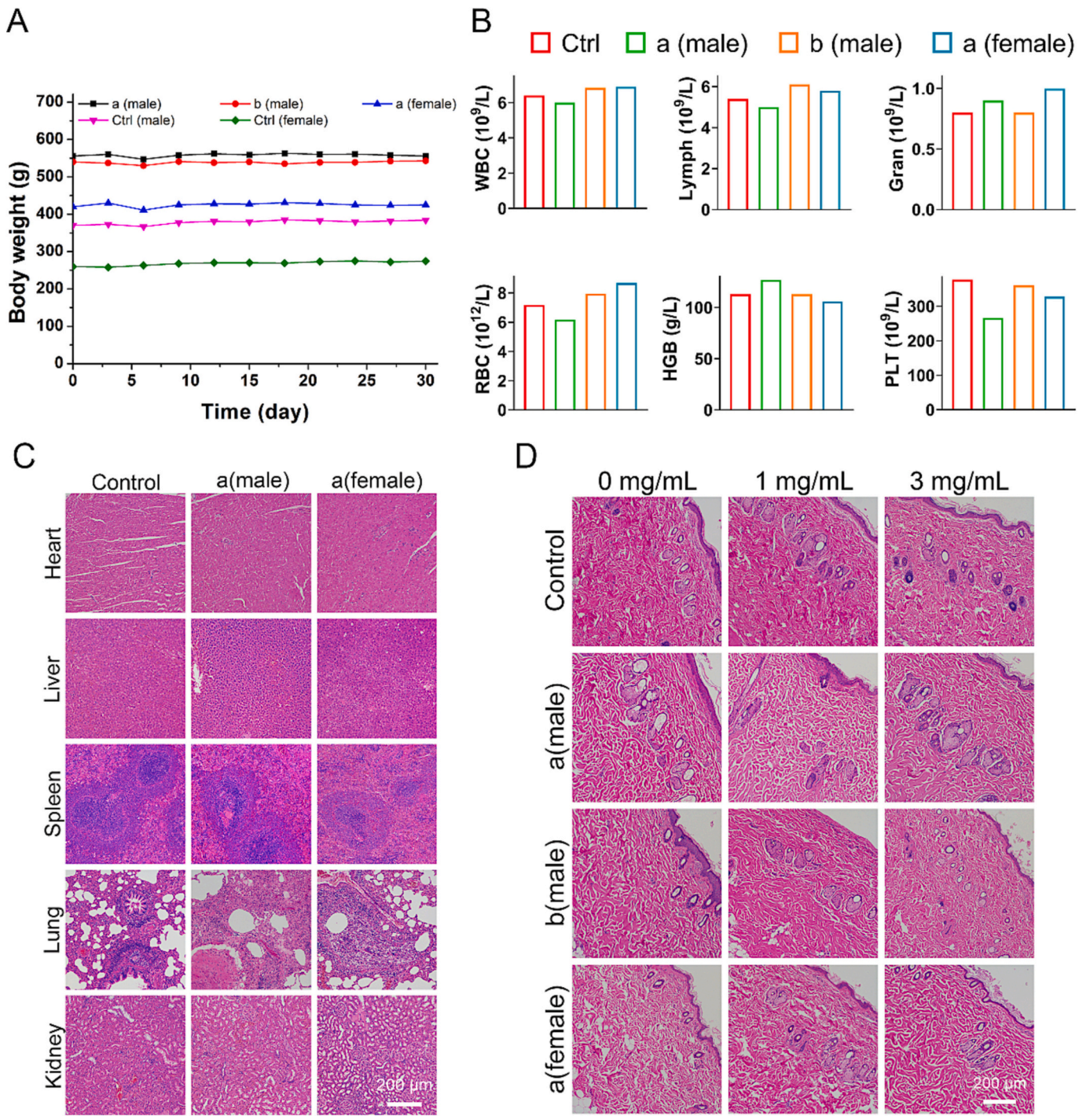

Fig. 5. (A) Weight analysis of rats. (B) Blood routine examination of rats. (C) Hype staining in the main organs of rats. (D) Hype staining of rat skin.

To further confirm the mechanism by which porcine skin collagen delays senescence in HSF cells, p53 and p16 protein levels were analyzed. As shown in Fig. 4F–H, Col I significantly decreased the protein expression of p53 and p16, in agreement with our immunofluorescence results. Meanwhile, the expression of p53 and p16 in the experimental group was much lower than that in the positive control group and was close to that of the control group, which indicated that Col I had a better effect than Col III in delaying the senescence of HSF cells by reducing the expression of senescence-related proteins. The results indicated that porcine skin collagen could provide a good extracellular environment for the growth of HSF cells and inhibit the intracellular MAPK cascade and the p53 pathway, thus blocking G1 cell cycle arrest and delaying senescence of HSF cells.

3.8. Biosafety and good biocompatibility of porcine skin collagen

To further verify the biological safety of porcine skin collagen *in vivo*, the body weight of rats after intervention was determined (Fig. 5A). During a period of one month of injection treatment, the body weight of old and young rats fluctuated little, and there was no significant difference. As shown in Fig. 5B, compared with the rats in the control group (injected with normal saline only), there was no significant difference in the blood routine indexes of rats in the experimental group (injected with collagen), and all of them were within the normal range.

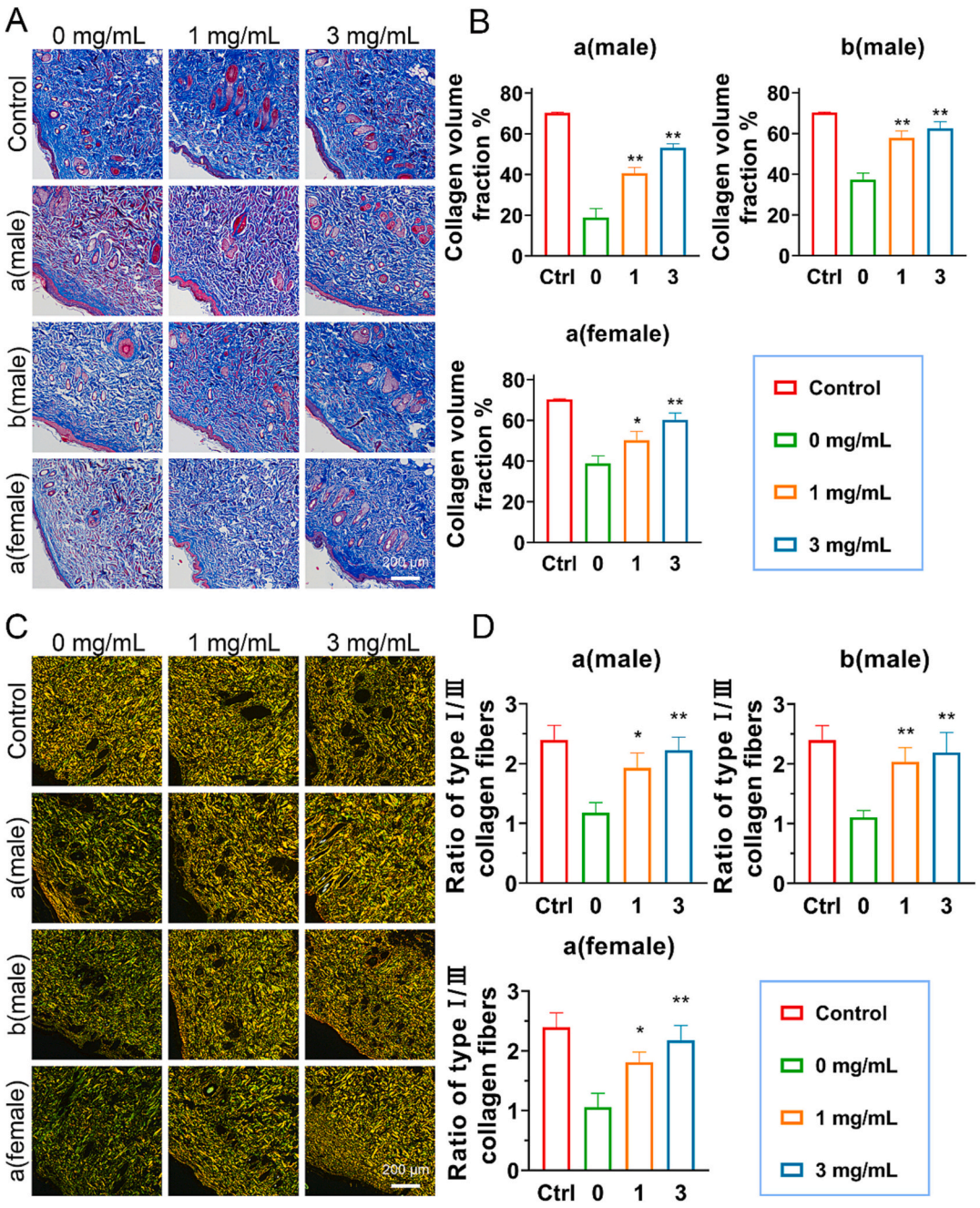

Fig. 6. (A) Masson staining and (B) quantitative analysis of collagen in dermis after local treatment ($n = 4$, $^{*}p < 0.05$ and $^{**}p < 0.01$). (C) Sirius red staining and (D) analysis of the proportion of type I and III collagen in dermis of rats after local treatment ($n = 4$, $^{*}p < 0.05$ and $^{**}p < 0.01$).

To verify whether porcine skin collagen is toxic and accumulates in rats, the main organs of rats were extracted, sliced, and stained to observe whether there were toxic side effects on the organs. The staining results are shown in Fig. 5C. One month after injection of porcine skin collagen, the tissue morphology of organs in the experimental group was normal, and the cells were arranged in close order, and there was no difference compared with the control group. This shows that after injection, porcine skin collagen does not accumulate in the main organs and does not produce physiological toxicity. To sum up, porcine skin collagen has excellent biological safety. The data proved that after injection, porcine skin collagen does not cause inflammation or affect the growth of rats, indicating that it is safe and biocompatible.

3.9. Porcine skin collagen improved the skin of old rats

To investigate whether porcine skin collagen can delay skin aging, rat skin after collagen intervention was stained pathologically. As shown in Fig. 5D, compared with the young rats in the control group, the local epidermis of rats in the experimental group injected with normal saline was thickened, the cells in the dermis were twisted, and the intercellular space was enlarged, which indicated the senescence of rat skin. When porcine skin collagen was injected into the skin of aging rats, compared with the skin injected with normal saline, it was found that the number of dermal fibroblasts was increased, the arrangement of cells became tighter, and cell morphology basically returned to normal. The thickness of the epidermis was also decreased. With higher amounts of injected collagen, the epidermis and dermis improved more obviously. In all, porcine skin collagen helps to delay the aging of rat skin, and higher

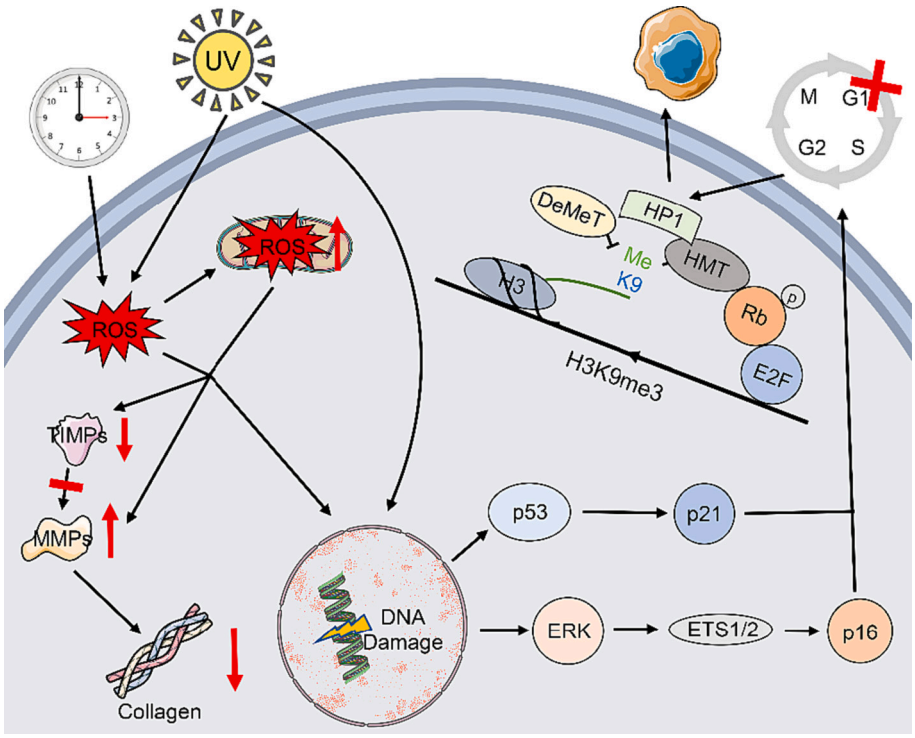

Fig. 7. Collagen provides a good extracellular environment for the growth of HSF cells, normalizes cell proliferation and interferes with cell senescence, reduces the accumulation of ROS in cells, reduces intracellular oxidative stress, thereby alleviates the effect of DDR, inhibits intracellular mitogen-activated protein kinase signal cascades (involving extracellular signal-regulated kinases (ERK) and ETS1/2) and the occurrence of p53 pathway. Thus, it can slow down the occurrence of G1 cell cycle arrest of HSF cells and delay the senescence of HSF cells.

amounts exert more significant anti-aging effects.

3.10. Porcine skin collagen promoted the type I collagen fibers in the skin of old rats

As shown in Fig. 6A & B, there were more collagen fibers, with a uniform and orderly structure, arranged horizontally in the dermis in young rats (control group). In the aging skin of old rats, the collagen fibers were arranged in disorder, and the gap between the collagen fibers was larger. After porcine skin collagen injection for one month, the collagen fibers in the dermis of aging rats increased significantly and were uniform and orderly. Porcine skin collagen can stimulate the formation of collagen fibers in the dermis of aging rats and promote remodeling of the extracellular matrix so as to delay skin aging.

Additionally, as shown in Fig. 6C & D, the Sirius red staining assay showed that the proportion of type I collagen fibers in young skin is about 2.4 times of that in type III fibers. The proportion of type I collagen fibers in aging skin decreased significantly. After local treatment, the proportion of type I and type III collagen fibers increased significantly, indicating that porcine skin collagen effectively promoted the production of type I collagen fibers in rat skin. It can be seen from the figure that the arrangement of collagen fibers becomes closer, and with the increase of the injected amount, the therapeutic effect is more obvious. In summary, porcine skin collagen mainly stimulates the production of type I collagen fibers in the dermis of aging rats to reshape the extracellular matrix, so as to delay skin aging (Fig. 7).

4. Conclusion

Porcine skin collagen could effectively promote the adhesion and chemotaxis of HSF cells and provide a good extracellular environment for cell growth. Porcine skin collagen could effectively alleviate cell senescence *in vitro*. In old rats, the thickness of the epidermis decreased and the number of dermal fibroblasts increased to restore cell morphology. The number of type I collagen fibers was significantly increased and the arrangement was more uniform and orderly. Porcine skin collagen has no obvious toxicity and is biocompatible. Therefore, porcine skin collagen might serve as a medical and cosmetic material to delay skin aging.

CRediT authorship contribution statement

He Ni: Investigation, Writing – original draft. **Chao Liu:** Methodology, Data curation. **Lili Kong:** Resources. **Limin Zhai:** Formal analysis. **Jiapeng Chen:** Formal analysis. **Qingpeng Liu:** Formal analysis. **Zhendong Chen:** Visualization. **Mengdie Wu:** Visualization. **Jie Chen:** Visualization. **Yiyan Guo:** Visualization. **Weiwei Bai:** Resources. **Dandan Zhang:** Resources. **Kunwen Xia:** Resources. **Guowei Huang:** Resources. **Shengjun Pan:** Resources. **Beining Liao:** Resources. **Kuo Ma:** Resources. **Ling-Kun Zhang:** Writing – review & editing. **Jian Cheng:** Funding acquisition, Supervision. **Yan-Qing Guan:** Project administration, Supervision.

Declaration of competing interest

The authors declare that they have no known competing financial interests or personal relationships that could have appeared to influence the work reported in this paper.

Acknowledgments

The expenses of this work were supported by the National Natural Science Foundation of China (31370967), the Guangdong Province Universities and Colleges Pearl River Scholar Funded Scheme (2014), China, the Horizontal subject of Zhejiang Sigenkell Biotechnology Co., Ltd, China, the Science and Technology Project of Guangzhou (202201010608), China.

References

[1] M.D. Shoulders, R.T. Raines, Collagen structure and stability, Annu. Rev. Biochem. 78 (2009) 929–958.
[2] K. Gelse, E. Pöschl, T. Aigner, Collagens—structure, function, and biosynthesis, Adv. Drug Deliv. Rev. 55 (12) (2003) 1531–1546.

[3] M. Egbert, M. Ruetze, M. Sattler, H. Wenck, S. Gallinat, R. Lucius, J.M. Weise, The matricellular protein periostin contributes to proper collagen function and is downregulated during skin aging, J. Dermatol. Sci. 73 (1) (2014) 40–48.
[4] D.H. Lee, J.H. Oh, J.H. Chung, Glycosaminoglycan and proteoglycan in skin aging, J. Dermatol. Sci. 83 (3) (2016) 174–181.
[5] A. Kammeyer, R.M. Luiten, Oxidation events and skin aging, Ageing Res. Rev. 21 (2015) 16–29.
[6] Y. Liu, Y. Liao, S. Wei, H. Zhang, X. Wang, Nanoparticles based on sodium alginate and β-conglycinin: self-assembly and delivery of Phyllanthus urinaria phenolic compounds, J. Food Process. Preserv. 43 (1) (2019), e13851.
[7] J. Varani, L. Schuger, M.K. Dame, C. Leonard, S.E. Fligiel, S. Kang, G.J. Fisher, J. J. Voorhees, Reduced fibroblast interaction with intact collagen as a mechanism for depressed collagen synthesis in photodamaged skin, J. Investig. Dermatol. 122 (6) (2004) 1471–1479.
[8] C.C. Zouboulis, E. Makrantonaki, G. Nikotakis, When the skin is in the center of interest: an aging issue, Clin. Dermatol. 37 (4) (2019) 296–305.
[9] K.M. Reiser, J.A. Last, Biosynthesis of collagen crosslinks: in vivo labelling of neonatal skin, tendon, and bone in rats, Connect. Tissue Res. 14 (4) (1986) 293–306.
[10] L. Rittié, A. Berton, J.-C. Monboisse, W. Hornebeck, P. Gillery, Decreased contraction of glycated collagen lattices coincides with impaired matrix metalloproteinase production, Biochem. Biophys. Res. Commun. 264 (2) (1999) 488–492.
[11] G.J. Fisher, J. Varani, J.J. Voorhees, Looking older: fibroblast collapse and therapeutic implications, Arch. Dermatol. 144 (5) (2008) 666–672.
[12] M. Man, S. Xin, S. Song, S. Cho, X. Zhang, C. Tu, K. Feingold, P. Elias, Variation of skin surface pH, sebum content and stratum corneum hydration with age and gender in a large Chinese population, Skin Pharmacol. Physiol. 22 (4) (2009) 190–199.
[13] P. Meyer, P. Maity, A. Burkovski, J. Schwab, C. Mussel, K. Singh, F.F. Ferreira, L. Krug, H.J. Maier, M. Wlaschek, T. Wirth, H.A. Kestler, K. Scharffetter-Kochanek, A model of the onset of the senescence associated secretory phenotype after DNA damage induced senescence, PLoS Comput. Biol. 13 (12) (2017), e1005741.
[14] F.P. Beserra, L.F.S. Gushiken, A.J. Vieira, D.A. Bergamo, P.L. Bergamo, M.O. de Souza, C.A. Hussni, R.K. Takahira, R.H. Nobrega, E.R.M. Martinez, C.J. Jackson, G. L.D. Maia, A.L. Rozza, C.H. Pellizzon, From inflammation to cutaneous repair: topical application of lupeol improves skin wound healing in rats by modulating the cytokine levels, NF-kappa B, Ki-67, growth factor expression, and distribution of collagen fibers, Int. J. Mol. Sci. 21 (14) (2020).
[15] J. Campisi, P. Kapahi, G.J. Lithgow, S. Melov, J.C. Newman, E. Verdin, From discoveries in ageing research to therapeutics for healthy ageing, Nature 571 (7764) (2019) 183–192.
[16] A.S. Wang, O. Dreesen, Biomarkers of cellular senescence and skin aging, Front. Genet. 9 (2018) 247.
[17] E.D. Lephart, Skin aging and oxidative stress: equol's anti-aging effects via biochemical and molecular mechanisms, Ageing Res. Rev. 31 (2016) 36–54.
[18] T. Quan, E. Little, H. Quan, J.J. Voorhees, G.J. Fisher, Elevated matrix metalloproteinases and collagen fragmentation in photodamaged human skin: impact of altered extracellular matrix microenvironment on dermal fibroblast function, J. Invest. Dermatol. 133 (5) (2013) 1362.
[19] U. Yokose, A. Hachiya, P. Sriwiriyanont, T. Fujimura, M.O. Visscher, W. J. Kitzmiller, A. Bello, R. Tsuboi, T. Kitahara, G.P. Kobinger, The endogenous protease inhibitor TIMP-1 mediates protection and recovery from cutaneous photodamage, J. Investig. Dermatol. 132 (12) (2012) 2800–2809.
[20] G.J. Fisher, T. Quan, T. Purohit, Y. Shao, M.K. Cho, T. He, J. Varani, S. Kang, J. J. Voorhees, Collagen fragmentation promotes oxidative stress and elevates matrix metalloproteinase-1 in fibroblasts in aged human skin, Am. J. Pathol. 174 (1) (2009) 101–114.
[21] S. Huang, D.E. Ingber, The structural and mechanical complexity of cell-growth control, Nat. Cell Biol. 1 (5) (1999) E131–E138.
[22] W. Huang, B. Anvari, J.H. Torres, R.G. LeBaron, K.A. Athanasiou, Temporal effects of cell adhesion on mechanical characteristics of the single chondrocyte, J. Orthop. Res. 21 (1) (2003) 88–95.
[23] F. Lacarrubba, A. Tedeschi, B. Nardone, G. Micali, Mesotherapy for skin rejuvenation: assessment of the subepidermal low-echogenic band by ultrasound evaluation with cross-sectional B-mode scanning, Dermatol. Ther. 21 (2008) S1–S5.
[24] R.J. Sage, M.C. Lopiccolo, A. Liu, B.H. Mahmoud, E.P. Tierney, D.J. Kouba, Subcuticular incision versus naturally sourced porcine collagen filler for acne scars: a randomized split-face comparison, Dermatol. Surg. 37 (4) (2011) 426–431.
[25] J.H. Lee, Y.S. Choi, S.M. Kim, Y.J. Kim, J.W. Rhie, Y.J. Jun, Efficacy and safety of porcine collagen filler for nasolabial fold correction in Asians: a prospective multicenter, 12 months follow-up study, J. Korean Med. Sci. 29 (Suppl. 3) (2014) S217–S221.
[26] K. Silvipriya, K.K. Kumar, A. Bhat, B.D. Kumar, A. John, Collagen: animal sources and biomedical application, J. Appl. Pharm. Sci. 5 (3) (2015) 123–127.
[27] R. Holmes, S. Kirk, G. Tronci, X.B. Yang, D. Wood, Influence of telopeptides on the structural and physical properties of polymeric and monomeric acid-soluble type I collagen, Mater. Sci. Eng. C Mater. Biol. Applic. 77 (2017) 823–827.
[28] M. Rafat, M. Jabbarvand, N. Sharma, M. Xeroudaki, S. Tabe, R. Omrani, M. Thangavelu, A. Mukwaya, P. Fagerholm, A. Lennikov, F. Askarizadeh, N. Lagali, Bioengineered corneal tissue for minimally invasive vision restoration in advanced keratoconus in two clinical cohorts, Nat. Biotechnol. 41 (1) (2023) 70–81.
[29] A.M. Carvalho, A.P. Marques, T.H. Silva, R.L. Reis, Evaluation of the potential of collagen from codfish skin as a biomaterial for biomedical applications, Mar. Drugs 16 (12) (2018).
[30] J. Qian, Y. Okada, T. Ogura, K. Tanaka, S. Hattori, S. Ito, J. Satoh, T. Takita, K. Yasukawa, Kinetic analysis of the digestion of bovine type I collagen telopeptides with porcine pepsin, J. Food Sci. 81 (1) (2016) C27–C34.
[31] K. Sato, T. Ebihara, E. Adachi, S. Kawashima, S. Hattori, S. Irie, Possible involvement of aminotelopeptide in self-assembly and thermal stability of collagen I as revealed by its removal with proteases, J. Biol. Chem. 275 (33) (2000) 25870–25875.
[32] X. Cao, Y. Wang, C. Wu, X. Li, Z. Fu, M. Yang, W. Bian, S. Wang, Y. Song, J. Tang, X. Yang, Cathelicidin-OA1, a novel antioxidant peptide identified from an amphibian, accelerates skin wound healing, Sci. Rep. 8 (1) (2018) 943.
[33] J.J. Zhang, X.X. Ma, D.D. Fan, C.H. Zhu, J.J. Deng, J.F. Hui, P. Ma, Synthesis and characterization of hyaluronic acid/human-like collagen hydrogels, Mater. Sci. Eng. C Mater. Biol. Applic. 43 (2014) 547–554.
[34] K. Wolf, S. Alexander, V. Schacht, L.M. Coussens, U.H. von Andrian, J. van Rheenen, E. Deryugina, P. Friedl, Collagen-based cell migration models in vitro and in vivo, Semin. Cell Dev. Biol. 20 (8) (2009) 931–941.
[35] J. Varani, M.K. Dame, L. Rittie, S.E.G. Fligiel, S. Kang, G.J. Fisher, J.J. Voorhees, Decreased collagen production in chronologically aged skin - roles of age-dependent alteration in fibroblast function and defective mechanical stimulation, Am. J. Pathol. 168 (6) (2006) 1861–1868.
[36] L. Eckhart, E. Tschachler, F. Gruber, Autophagic control of skin aging, Front. Cell Dev. Biol. 7 (2019) 143.
[37] G.Z. Li, M.S. Eller, R. Firoozabadi, B.A. Gilchrest, Evidence that exposure of the telomere 3′ overhang sequence induces senescence, Proc. Natl. Acad. Sci. U. S. A. 100 (2) (2003) 527–531.
[38] F. Rodier, J. Campisi, Four faces of cellular senescence, J. Cell Biol. 192 (4) (2011) 547–556.
[39] P.F. Da Silva, B. Schumacher, DNA damage responses in ageing, Open Biol. 9 (11) (2019), 190168.
[40] U. Panich, G. Sittithumcharee, N. Rathviboon, S. Jirawatnotai, Ultraviolet radiation-induced skin aging: the role of DNA damage and oxidative stress in epidermal stem cell damage mediated skin aging, Stem Cells Int. 2016 (2016), 7370642.